CrystEngComm

Crystallization and disorder of the polytypic α1 and α2 polymorphs of piroxicam

Journal:	*CrystEngComm*
Manuscript ID:	CE-ART-01-2015-000050.R1
Article Type:	Paper
Date Submitted by the Author:	23-Feb-2015
Complete List of Authors:	Upadhyay, Pratik; University of Copenhagen, Department of Pharmacy Bond, Andrew; University of Copenhagen, Department of Pharmacy

SCHOLARONE™
Manuscripts

Cite this: DOI: 10.1039/c0xx00000x

www.rsc.org/xxxxxx

ARTICLE TYPE

Crystallization and disorder of the polytypic α_1 and α_2 polymorphs of piroxicam

Pratik P. Upadhyay[a] and Andrew D. Bond*[a,b]

Received (in XXX, XXX) Xth XXXXXXXXX 20XX, Accepted Xth XXXXXXXXX 20XX

DOI: 10.1039/b000000x

Polymorphism of the active pharmaceutical ingredient piroxicam, $C_{15}H_{13}N_3O_4S$, is investigated with an aim to clarify the identity and crystallization conditions of the α_1 and α_2 polymorphs. The structures are polytypic, containing identical 2-dimensional layers, with different symmetry relationships between the layers. The α_1 structure is orthorhombic and non-centrosymmetric (space group type $Pca2_1$), while the α_2 structure is monoclinic and centrosymmetric (space group type $P2_1/c$). α_2 can be crystallized by evaporation from ethanol at 25°C, while α_1 is obtained by crystallization from the same solvent at 4°C. The polytypic relationship provides a suitable condition for order-disorder phenomena to be observed in single crystals. Intermolecular interaction energies calculated using the *PIXEL* method suggest that the centrosymmetric interlayer regions in α_2 involving the pyridyl groups are more stabilising than the corresponding non-centrosymmetric interlayer regions in α_1. This is consistent with observations of inversion twinning in non-centrosymmetric α_1 crystals. The interlayer regions involving the benzothiazine groups have very similar interaction energies in the two structures.

Introduction

Piroxicam is a non-steroidal anti-inflammatory drug (NSAID) belonging to the class of oxicam.[1] Crystalline piroxicam is known to show polymorphism, which has been studied quite extensively since its discovery. The compound is established to crystallize in several anhydrous forms,[2–5] and one monohydrate form.[6] For the anhydrous compound, there are currently eight entries in the Cambridge Structural Database (CSD; Nov. 2013 release plus updates), which fall into four structural groups (Table 1). As is often the case for well-studied compounds, the nomenclature of the polymorphs in the primary literature is inconsistent. The situation up to 2004 was summarised in a helpful article by Sheth *et al*.[4] Form I (also called the β form) was the first structure to be described (CSD: BIYSEH),[2] and it crystallizes commonly by slow cooling from various solvents. Form III was observed by Vrečer *et al.* in 2003,[7] and has been obtained by rapid pouring of hot saturated solutions onto dry ice[7] or by spray drying.[5] The crystal structure of form III was determined from powder X-ray diffraction (PXRD) data in 2012 (BIYSEH07).[5]

The subject of this paper is the polymorph originally labelled as the α form, and later (ambiguously) re-labelled as form II.[8] An orthorhombic crystal structure was first reported from single-crystal data in 1988 by Reck *et al.* (BIYSEH02).[3] In that paper, the authors noted that Weissenberg photographs contained diffuse strips and a few weak additional reflections, which led them to propose an order-disorder (OD) model,[9] with the orthorhombic form being one maximum-degree-of-order (MDO) structure. On the basis of the OD model, a monoclinic structure corresponding to a second MDO structure was deduced.[10] The orthorhombic and monoclinic structures were labelled α_1 and α_2, respectively, and they are polytypes.[11] Reck *et al*. initially showed the existence of α_1 and α_2 by comparing to measured PXRD patterns, and they noted that the α_1 and α_2 structures frequently appear in varying ratios in bulk samples. A single-crystal structure for α_2 was later determined by Vrečer *et al.* (BIYSEH06),[7] where the authors refer to it as form II.

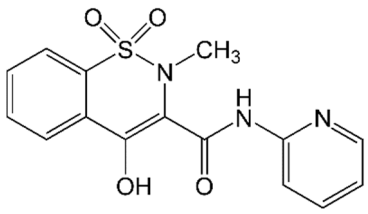

Scheme 1 Molecular structure of piroxicam

Although the polytypic relationship and probable disordered nature of α_1 and α_2 was described by Reck *et al.* in 1990,[10] the identity of the polymorphs does not seem to be clear in the subsequent literature. This is possibly because of the close structural relationship between the polytypes or perhaps because of the introduction of the ambiguous form II label by Vrečer *et al*.[7] The summary article by Sheth *et al.* is unclear on this point: it states that "*...form II has also been named α, α_1, α_2...*",[4] which indicates that all three α labels refer to the same "form II". In this article, we aim to clarify the existence and identity of the piroxicam polymorphs α_1 and α_2, by describing their polytypic relationship and by identifying reproducible crystallization conditions for both. The structural situation is comparable to that described for aspirin, which exhibits intergrowth polymorphism

on account of the polytypic relationship between forms I and II.[12,13] A similar situation has also been shown for felodipine, where crystals reported to be form II comprise domains of two polytypes.[14] In this paper, we retain the original piroxicam α_1/α_2 notation of Reck *et al.* for consistency with the original work.

Table 1 CSD entries for anhydrous piroxicam

Polymorph	CSD Refcode	Symmetry and approximate unit-cell parameters (Å, °)	Ref.
Form I (= β form)	BIYSEH BIYSEH01 BIYSEH03 BIYSEH04	Monoclinic, $P2_1/c$ a = 7.1, b = 15.1, c = 13.9, β = 97.4	[2] [15] [4] [4]
α_1	BIYSEH02	Orthorhombic, $Pca2_1$ a = 11.8, b = 17.4, c = 7.0	[3]
α_2	BIYSEH05 BIYSEH06	Monoclinic, $P2_1/c$ a = 17.6, b = 11.9, c = 7.0 β = 97	[4] [7]
Form III	BIYSEH07	Triclinic, P–1 a = 8.0, b = 10.1, c = 10.5 α = 81.2, β = 69.3, γ = 69.8	[5]

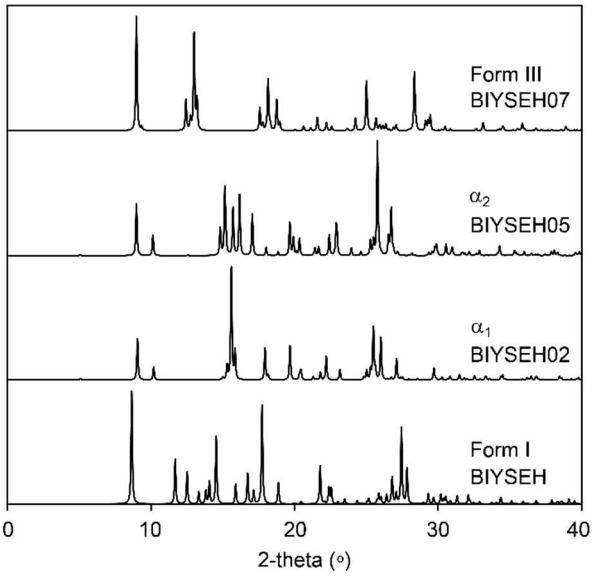

Fig. 1 Simulated powder X-ray diffraction patterns (CuKα_1 radiation, λ = 1.5406 Å) for piroxicam structures in the CSD. All patterns are based on crystal structures determined at room temperature.

Materials and Methods

Piroxicam (USP32) was purchased from Chr. Olesen Pharmaceuticals A/S (Gentofte, Denmark) and was found to be Form I by PXRD. All solvents used were of HPLC grade with purity ≥99.8 %.

Crystallization experiments

Crystallization experiments were set up at concentrations 2.0, 5.0, 10.0 and 15.0 mg/mL in various solvents as listed in Table 2. The samples at 2.0 mg/mL were sonicated for 10 mins in order to obtain a clear solution. At 5.0 mg/mL in methanol, ethanol, acetonitrile and *n*-propanol, a suspension was formed upon sonication, which was further heated to 50°C to obtain a clear solution. At 10.0 and 15.0 mg/mL, all samples except for acetone, dichloromethane, dimethylsulfoxide and dimethylacetamide formed a suspension and were heated to obtain a clear solution. All hot solutions were cooled slowly to room temperature (preventing rapid crashing) and left to evaporate at either 25 or 4°C.

X-Ray Diffraction

Single-crystal X-ray diffraction data were collected on a Bruker D8-QUEST instrument, equipped with a PHOTON-100 detector and an Incoatec IμS microsource (CuKα radiation; λ = 1.5418 Å) at 298 K. Data collection and reconstruction of precession images were carried out using the *APEX2* package.[16] Powder X-ray diffraction data were collected on a Panalytical X'Pert Pro instrument, equipped with a PIXcel detector using non-monochromated CuKα radiation (λ = 1.5418 Å). The sample was placed in a zero-background Si holder and measured in reflection geometry with sample spinning. Samples were ground thoroughly before mounting in an effort to minimise preferred orientation. The PXRD patterns were fitted by Pawley refinement using *TOPAS Academic*,[17] starting from the unit-cell parameters of BIYSEH02 (α_1) and BIYSEH05 (α_2).

Computational Methods

Energy minimisation of the crystal structures was carried out using the *CASTEP* module[18] in *Materials Studio*.[19] The starting structures were BIYSEH05 (α_2) and a transformed version of BIYSEH02 (α_1) as described in the Results and Discussion section. The PBE functional was applied[20] with a plane-wave cut-off energy of 520 eV and a dispersion correction according to Grimme.[21] All other parameters were set to the "fine" defaults within *Materials Studio*; full details are included in the ESI†. All atomic coordinates and unit-cell parameters were optimized.

Results and Discussion

Crystallization studies

We have crystallized piroxicam under various conditions and solvents, as summarized in Table 2, with an emphasis on targeting the α_1 and α_2 forms. Numerous other authors have reported piroxicam crystallization results, so the following discussion compares to the published results where relevant.

Michalić *et al.* were first to describe the crystallization behaviour in ethanol in 1982.[1] They stated that fast cooling of saturated ethanolic solutions leads to the "needle form" whereas slow cooling produces the "cubic form". The "cubic form" is identifiable as form I, but it is difficult to identify the "needle form" conclusively as either α_1 or α_2. The published PXRD pattern matches most closely with α_1, but the stated melting point (196–198°C) matches with α_2 (according to our DSC results). In 1999, Csóka *et al.* also obtained "white needle crystals" from ethanol, with a melting point that indicates α_2.[22] We find that slow evaporation from ethanol gives initially α_2 as needles, but that these needles convert to form I over 1–2 weeks on standing in the same solution. The $\alpha_2 \rightarrow$ I conversion appeared to take place more rapidly for the lower solution concentrations (*ca* 5 mg/mL) than at the higher concentrations.

This journal is © The Royal Society of Chemistry [year]

Table 2 Summary of crystallization results for piroxicam in selected solvents and conditions.[a] Polymorph identity is established by unit-cell determination on selected single crystals and by PXRD of the bulk

	Slow evap. at 25°C	Slow evap. at 4°C
Ethanol	α_2	α_1
Acetone	I + α_2	α_1
Methanol	I + α_1	α_1
Isopropyl acetate	I + α_2	α_1
Ethyl acetate	I + α_2	
n-Propanol	α_2	
Acetonitrile	I	
Chloroform	I	
Toluene	I	
Dichloromethane	I	
Dimethylsulfoxide[b]	I	
Dimethylacetamide[b]	I	

[a] All solvents are anhydrous. The presence of water leads readily to crystallization of piroxicam monohydrate.

[b] α_2 obtained by crash cooling of hot solutions to room temperature.

In 1991, Janik *et al.* studied the influence of various solvents on the crystallization behaviour, and reported that the "α structure" crystallized from ethanol, isopropanol, THF, acetonitrile and chloroform.[23] We find some conflicting results: we observe that form I crystallizes as large rods from acetonitrile or chloroform under slow evaporation at 25°C. However, the conclusions of Janik *et al*. were made solely on the basis of IR spectra, without measurement of PXRD patterns, so the effectiveness of their polymorph identification may be in doubt.

Also in 1991, Vrečer *et al.* produced α_1 by crash cooling of methanol, ethanol, acetone, *n*-propanol or chloroform solutions.[8] The identity of α_1 is clear from the published DSC traces (compared to our DSC traces reported herein), but accompanying PXRD data were not reported and the authors did not make any distinction between α_1 and α_2. Indeed, they refer to "form II" in their 1991 paper for obtained α_1 samples, but in 2003 refer again to "form II" for samples that are clearly α_2. We observe that α_1 is obtained exclusively and reproducibly by slow evaporation of piroxicam solutions in ethanol, methanol, acetone or isopropyl acetate at reduced temperature (around 4°C). As seen in SEM images (Fig. 2), α_1 crystallizes as fine needles. The PXRD patterns of the bulk crystallized materials (Fig. 3) match well with the pattern simulated from BIYSEH02.

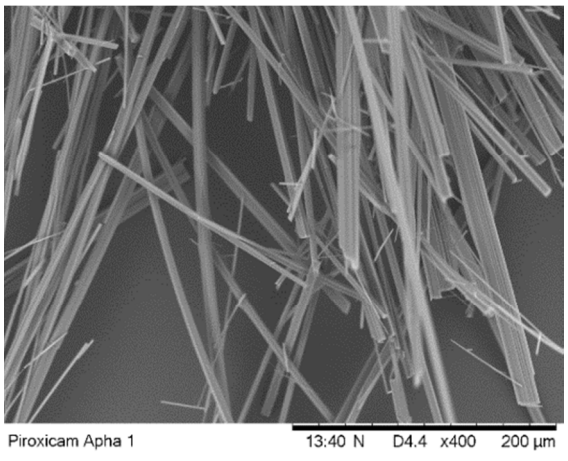

Fig. 2 SEM image of α_1 crystals, showing the fine needle morphology.

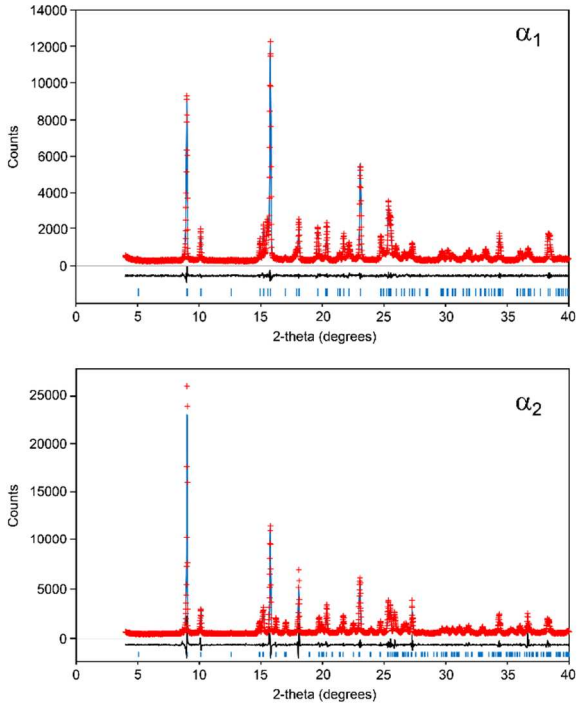

Fig. 3 Pawley fits to PXRD patterns (non-monochromated CuKα radiation, λ = 1.5418 Å) measured for bulk samples of α_1 and α_2. Refined unit-cell parameters: α_1, *Pbc*2$_1$, *a* = 17.4120(7), *b* = 11.8350(4), *c* = 6.9871(5) Å; α_2, *P*2$_1$/*c*, *a* = 17.6122(10), *b* = 11.8758(6), *c* = 6.9571(6) Å, β = 97.474(12)°.

In summary: we find that α_1 can be crystallized reproducibly from ethanol, methanol, acetone or isopropylacetate at 4°C, while α_2 crystallizes from ethanol at 25°C, but undergoes solvent-mediated transformation to form I if left in contact with the crystallization solution.

Crystal structures of α_1 and α_2

To enable a direct comparison between the crystal structures of α_1 and α_2, we transform the published structure of BIYSEH02 (α_1) using the matrix [0 1 0 / –1 0 0 / 0 0 1] to give unit-cell parameters *a* = 17.4, *b* = 11.8, *c* = 7.0 Å in the non-standard space group setting *Pbc*2$_1$. H atoms are not included in BIYSEH02, but can be unambiguously added in geometrical positions. This transformed structure of BIYSEH02 is compared below to the CSD entry BIYSEH05 (α_2).

The two structures contain identical layers in the *bc* planes, but the *a* axis (the long axis) is aligned differently. The orthorhombic unit cell of α_1 can be transformed to the monoclinic unit cell of α_2 by application of the transformation matrix [1 0 ⅓ / 0 1 0 / 0 0 1], which corresponds to shearing of the unit cell parallel to the *c* axis, *i.e.* $\boldsymbol{a}(\alpha_2) = \boldsymbol{a}(\alpha_1) + \frac{1}{3}\boldsymbol{c}(\alpha_1)$. In projection along the *c* axis, the structures appear identical (Fig. 4). The difference is seen in projection along the *b* axis (Fig. 4). The layers in α_1 are related by 2$_1$ screw axes parallel to *c*, and by *b*- and *c*-glides perpendicular to the *a* and *b* axes, respectively The structure is non-centrosymmetric and polar, with all N–CH$_3$ vectors pointing in the same direction along the *c* axis. In the α_2 structure, inversion centres exist between the layers. The two alternative orientations for a given layer are related to each other by a mirror operation perpendicular to the *c* axis (Fig. 5).

There are two different interlayer regions: one where the pyridyl rings meet (at the upper and lower edges of the unit cell drawn in Fig. 4), and one where the benzothiazine ends of the molecules meet (at the middle of the unit cell in Fig. 4). In both regions, the local intermolecular relationships are mirrored, but the contacts remain similar. The principal interactions are C—H···O from the pyridyl and benzothiazine rings to the O atoms of the S=O, C=O and C—OH groups. The intermolecular interactions and their energies are discussed in more detail subsequently.

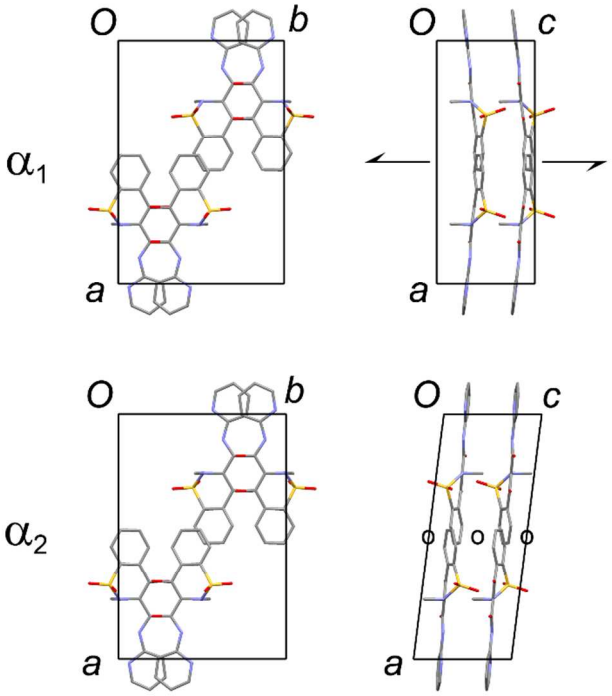

Fig. 4 Unit cells of the α_1 and α_2 structures. The structures look identical in projection along the *c* axis (left), but different in projection along the *b* axis (right). The consistent layers are in the *bc* planes (horizontal). α_1 is non-centrosymmetric and polar (all N–CH_3 groups point in the same direction along *c*), while α_2 is centrosymmetric. H atoms are not shown.

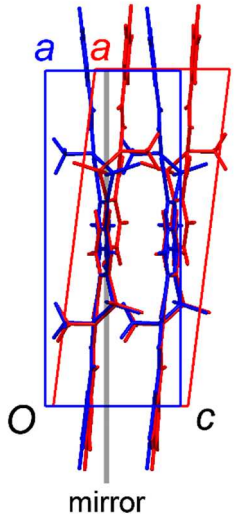

Fig. 5 Overlay of α_1 (blue) and α_2 (red) showing the mirror relationship between the alternative layer orientations.

Relationship between the diffraction patterns

One of our principal interests with the α_1 and α_2 piroxicam structures is their polytypic relationship and the potential for stacking faults and/or intergrowth polymorphism, similar to aspirin.[12,13] By considering the relationship between the single-crystal diffraction patterns of the two forms, we consider here how such phenomena would be observed. With the consistent layers in both structures lying in the *bc* planes, α_1 and α_2 have their *a** and *b** axes aligned, but not their *c** axes. The idealized geometry in the plane containing *a** and *c** is shown in Fig. 6. α_1 has an orthorhombic lattice with *c** perpendicular to *a**, and parallel to the *c* axis in real space (horizontal in Fig. 6). In α_2, *c** makes an angle of ~7° to this direction. The geometry is such that the diffraction spots along *a** for α_2 are offset by one third of the lattice spacing for α_1. This offset could occur in either direction, giving three sets of evenly-spaced diffraction spots along *a** (Fig. 6). Since the (idealized) offset between the spots is ⅓*a**, the lattices come back into coincidence in every third row along *c** (*i.e.* $l = 0, 3, 6$, *etc.*). This is also expressed by the transformation matrix relating the two unit cells: [1 0 ⅓ / 0 1 0 / 0 0 1]. The observation of three sets of discrete Bragg spots, as indicated in Fig. 6, would refer to a situation where the domain sizes of the three cases (α_1 + α_2 in two different orientations related by 180° rotation around the *c* axis) were suitably large. Smaller domain sizes, corresponding to more frequent turnover between domains, would generate diffuse streaks along *a** for $l \neq 0, 3, 6$, *etc.*

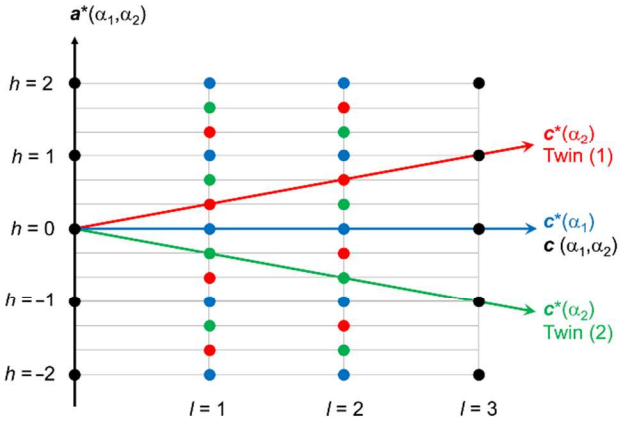

Fig. 6 Schematic illustration of the idealized geometry for the diffraction patterns of α_1 and α_2 in the *a***c** planes. Blue spots correspond to orthorhombic α_1. Red and green spots correspond to two orientations of monoclinic α_2, related to each other by 2-fold rotation around the real *c* axis (horizontal). The black spots are coincident in all three lattices.

Single-crystal X-ray diffraction

Crystals of α_1 obtained from ethanol at 4°C were studied by single-crystal X-ray diffraction. A representative reconstructed precession image for the *h*1*l* plane is shown in Fig. 7. In the image shown, faint diffuse streaks are visible along *a**, which give some indication of layer stacking disorder, but we have not observed any crystals with additional Bragg peaks that might indicate significant α_2 domains. Since the structure is non-centrosymmetric, the presence of one stacking fault corresponding to the inversion-related interlayer arrangement in α_2 would manifest itself as inversion twinning. We have found

This journal is © The Royal Society of Chemistry [year]

some crystals where the Flack parameter refines to zero (indicating no inversion twinning) and others where it refines to a non-zero value (with suitably small uncertainty) due to inversion twinning. Thus, twinning of the α_1 structure by incorporation of the α_2 interlayer arrangement is found to occur, but to date we have not observed any clear indications of sizeable α_2 domains within α_1 single crystals. A representative structure from our α_1 crystal has been deposited at the Cambridge Crystallographic Data Centre (CCDC 1050926).

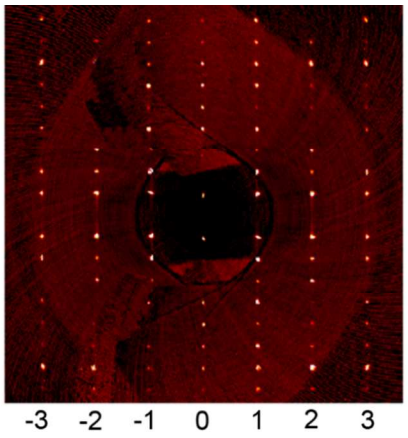

Fig. 7 Reconstructed *h*1*l* precession image for a representative crystal of α_1, aligned as in Fig. 6. Faint streaks are visible in the vertical direction.

Numerous crystals of α_2 were studied, and these were frequently found to be twinned. Using the unit cell established for α_2 in space group $P2_1/c$ ($a \approx 17.6$, $b \approx 11.9$, $c \approx 7.0$ Å, $\beta \approx 97°$), the relationship between the twin domains was established to be a 180° rotation around the *c* axis, as indicated in Fig. 6. A typical reconstructed precession image for the *h*1*l* plane is shown in Fig. 8. The Bragg reflections of the two twin components are clearly separated, and diffuse streaks indicate less ordered regions. The coincidence of the two lattices for $l = 3$ is apparent. The twin operation corresponds to introduction of the α_1 interlayer arrangement, but again we have not observed any clear indications of Bragg reflections corresponding to sizeable α_1 domains within α_2 single crystals. A representative α_2 structure has been deposited at the Cambridge Crystallographic Data Centre (CCDC 1050927).

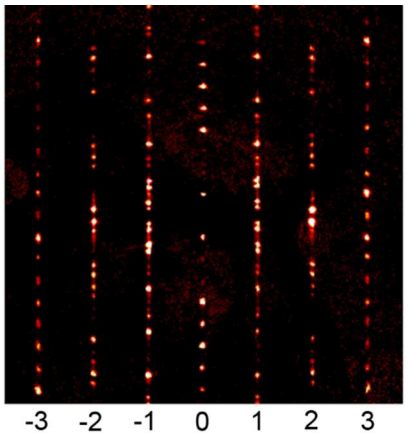

Fig. 8 Reconstructed *h*1*l* precession image for a representative crystal of α_2, aligned as in Fig. 6. Multiple Bragg peaks and diffuse streaks are evident in the vertical direction. The $l = 0$ and $l = 3$ rows appear normal.

Finally, it is interesting to note that twinned α_2 crystals indexed in a standard way commonly indicate $a \approx 52.3$ Å ($\approx 3 \times 17.6$ Å). The reason for this is clear from Figs. 6 and 8. A similar long axis was reported by Reck *et al.*[3] in their first determination of the α_1 structure, *i.e.* the *orthorhombic* form. This could indicate that their α_1 crystals contained sizeable domains of the α_2 structure (*i.e.* their diffraction pattern resembled the situation in Fig. 6). This would amount to intergrowth polymorphism, similar to the situation reported for aspirin[12,13] and felodipine form II.[14] We have not reproduced any such result to date, but it is clear from the polytypic relationship that there is potential for such a situation to exist.

Thermal analysis

Thermal analysis of bulk α_1 and α_2 was carried out by differential scanning calorimetry (DSC), with form I also measured for comparison (Fig. 9). Form I shows a single sharp melting endotherm with onset 201.2°C. α_2 also shows a single sharp melting endotherm with onset 198.8°C, which matches well with the α_2 melting point reported by Michalić *et al*. (196–198°C).[1] For α_1, a first endotherm is seen at 194.8°C, corresponding to melting, followed by an exotherm that corresponds to crystallization of form I then a subsequent melting endotherm for form I.

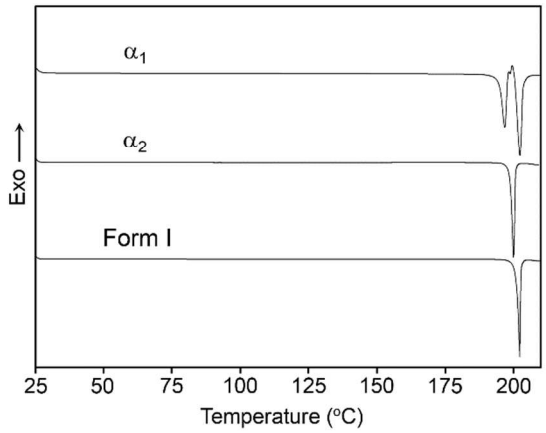

Fig. 9 DSC thermograms for bulk samples of form I, α_1 and α_2.

Intermolecular interaction energies

To obtain an indication of the relative stabilities of α_1 and α_2, the structures of BIYSEH02 (α_1) and BIYSEH05 (α_2) were energy-minimized using dispersion-corrected density functional theory calculations (DFT-D). Details and minimized structures are provided in the ESI.† The resulting energies (at 0 K) suggest that α_2 is moderately more stable than α_1, which is nominally consistent with the observed melting points. Pairwise intermolecular interaction energies were then calculated from the minimized structures using the *PIXEL* method (Table 3).[24] The total potential energy for a molecule in each structure is indistinguishable within the expected precision of these calculations. However, the distribution of the interactions is different. The results are visualised in Fig. 10 using energy-vector diagrams of the type developed by Shishkin and co-workers,[25] generated using the *processPIXEL* program.[26] Table 3 shows sums of the principal stabilising interactions partitioned into intra- and interlayer regions. The most striking result is that the

pyridyl interlayer region in the α_2 structure is calculated to be more stabilising than any of the other interlayer regions. This is mainly due to a particularly stabilising pairwise interaction between inversion-related molecules, with a substantial coulombic component originating from C—H···O interactions involving both SO_2 groups (Fig. 11). The corresponding non-centrosymmetric interaction in the α_1 structure involves only one such contact and is substantially less stabilising. If the twinning in both structures were to be controlled by the intermolecular interaction energies, Table 3 implies the following observations: (i) inversion twinning in the non-centrosymmetric α_1 structure is most likely to occur at the pyridyl interlayer region; (ii) twinning in the α_2 structure is most likely to occur at the benzothiazine interlayer region.

Table 3 Interaction energies (kJ·mol^{-1} per molecule) calculated for α_1 and α_2 using the *PIXEL* method, applied to DFT-D minimized structures. Full details are available in the ESI.†

Polymorph	Total	Intralayer	Interlayer pyridyl	Interlayer benzothiazine
α_1	–153.8	–53.7	–53.4	–38.9
α_2	–153.9	–52.7	–57.1	–39.9

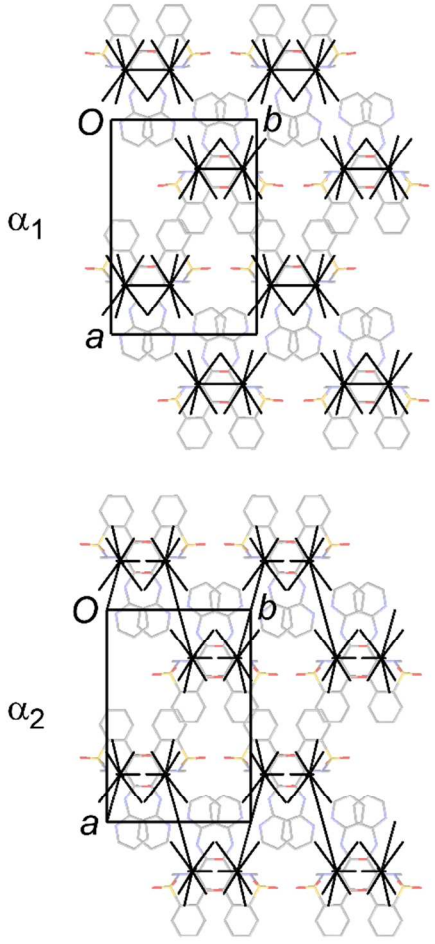

Fig. 10 Energy-vector diagrams representing the results of *PIXEL* calculations for α_1 and α_2. The most stabilising interaction in each structure is represented by a continuous line joining the centroids of the molecules. Other interactions are represented by discontinuous lines, with a larger gap indicating a less stabilising interaction.[25,26]

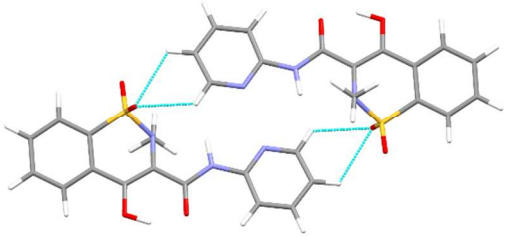

Fig. 11 The most stabilising pairwise intermolecular interaction in the α_2 structure: centrosymmetric, with C—H···O interactions (light blue lines) between the pyridyl rings and SO_2 groups.

Conclusions

With this clarification of the structures of piroxicam forms α_1 and α_2, and a specific report of crystallization conditions for both, piroxicam has four well-established polymorphs. We have chosen to retain the α_1/α_2 notation of Reck *et al.* in order to maintain consistency with the original work. Where the "form II" label introduced by Vrečer *et al.* is seen in the literature, it should be considered carefully whether the information in the paper is sufficient to distinguish α_1 from α_2. We have obtained single-crystal data that show that orthorhombic α_1 can exist with only minimal twinning/disorder, but single crystals that we have obtained for monoclinic α_2 have frequently been twinned. So far, we have not obtained any single crystals that show clear domains of both the α_1 and α_2 polymorphs simultaneously, as would be the case for intergrowth polymorphism.

This article certainly does not represent the end of the story for piroxicam polymorphism. We are currently aware of two additional crystal structures, one of which we have obtained during our solution crystallization experiments, and one of which has its unit-cell parameters and simulated PXRD pattern reported.[27] The latter is a high *Z′* form. There has also been a recent report of a further new form obtained from chloroform solution by electrospray methods,[28] and we have produced similar PXRD patterns in the course of our work. Thus, at least two more anhydrous piroxicam crystal structures are already known, and there appears to exist one other solid form whose structure is yet to be established. This will bring the known total (so far) up to seven polymorphs, making piroxicam one of the more prolific polymorphic pharmaceutical compounds.

Acknowledgements

This work was funded by the Danish Council for Independent Research | Natural Sciences (DFF-1323-00122).

Notes and references

[a] *University of Copenhagen, Department of Pharmacy, Universitetsparken 2, 2100 Copenhagen Ø, Denmark.*
[b] *Present address: University of Cambridge, Department of Chemistry, Lensfield Road, Cambridge, CB2 1EW, UK. Tel: +44 1223 336352; E-mail:adb29@cam.ac.uk.*

† Electronic Supplementary Information (ESI) available: details of the DFT and *PIXEL* calculations for α_1 and α_2. See DOI: 10.1039/b000000x/

1 M. Mihalić, H. Hofman, F. Kajfež, J. Kuftinec, N. Blažević and M. Žinić, *Acta Pharm. Jugosl.* 1982, **32**, 13.
2 B. Kojić-Prodić and Ž. Ružić-Toroš, *Acta Cryst.* 1982, **B38**, 2948.

This journal is © The Royal Society of Chemistry [year]

3 G. Reck, G. Dietz, G. Laban, W. Günther, G. Bannier and E. Höhne, *Pharmazie*, 1988, **43**, 477.

4 A. R. Sheth, S. Bates, F. X. Muller and D. J. W. Grant, *Cryst. Growth Des.* 2004, **4**, 1091.

5 K. Naelapää, J. van de Streek, J. Rantanen and A. D. Bond, *J. Pharm. Sci*, 2012, **101**, 4214.

6 J. Bordner, J. A. Richards, P. Weeks and E. B. Whipple, *Acta Cryst*. 1984, **C40**, 989.

7 F. Vrečer, M. Vrbinc and A. Meden, *Int. J. Pharm.* 2003, **256**, 3.

8 F. Vrečer and S. Srcic, *Int. J. Pharm.* 1991, **68**, 35.

9 K. Dornberger-Schiff, *Acta Cryst.* 1982, **A38**, 483.

10 G. Reck and G. Laban, *Pharmazie*, 1990, **45**, 257.

11 International Union of Crystallography, Online Dictionary of Crystallography, http://reference.iucr.org/dictionary/Polytypism

12 A. D. Bond, R. Boese and G. R. Desiraju, *Angew. Chem. Int. Ed.* 2007, **46,** 615.

13 A. D. Bond, R. Boese and G. R. Desiraju, *Angew. Chem. Int. Ed.* 2007, **46,** 618.

14 M. K. Mishra, G. R. Desiraju, U. Ramamurty, and A. D. Bond, *Angew. Chem. Int. Ed*. 2014, **53**, 13102.

15 I. H. Suh, K. J. Kim, T. S. Ko, B. H. Kim and C. K. Yong. *Chungnam J. Sci*. 1989, **16**, 30.

16 Bruker AXS, *APEX2*. Madison, Wisconsin, USA, 2013.

17 A. A. Coelho, *TOPAS Academic v. 4.1*. Coelho Software, Brisbane, Australia, 2007.

18 S. J. Clark, M. D. Segall, C. J. Pickard, P. J. Hasnip, M. J. Probert, K. Refson and M. C. Payne, *Z. Kristallogr.* 2005, **220**, 567.

19 Accelrys, *Materials Studio v. 6.0.* San Diego, California, USA, 2011.

20 J. P. Perdew, K. Burke and M. Ernzerhof, *Phys. Rev. Lett.* 1996, **77**, 3865.

21 S. Grimme, *J. Comput. Chem.* 2006, **27**, 1787.

22 G. Csóka, E. Balogh, S. Marton, E. Farkas and I. Rácz, *Drug. Dev. Ind. Pharm.* 1999, **25**, 813.

23 M. Janik, Z. Malarski, J. Mroziński, J. Wajcht and Z. Zborucki, *J. Cryst. Spect. Res.* 1991, **21**, 519.

24 A. Gavezzotti, *New J. Chem.* 2011, **35**, 1360.

25 O. V. Shishkin, V. V. Dyakonenko and A. V. Maleev, *CrystEngComm*, 2012, **14**, 1795.

26 A. D. Bond, *J. Appl. Cryst.* 2014, **47**, 1777.

27 C. Wales, Ph.D. Thesis, University of Glasgow, 2013.

28 M. Nyström, J. Roine, M. Murtomaa, R. M. Sankaran, H. A. Santos and J. Salonen, *Eur. J. Pharm. Biopharm*. doi:10.1016/j.ejpb.2014.11.027

Cite this: DOI: 10.1039/c0xx00000x

www.rsc.org/xxxxxx

ARTICLE TYPE

Table of Contents Entry

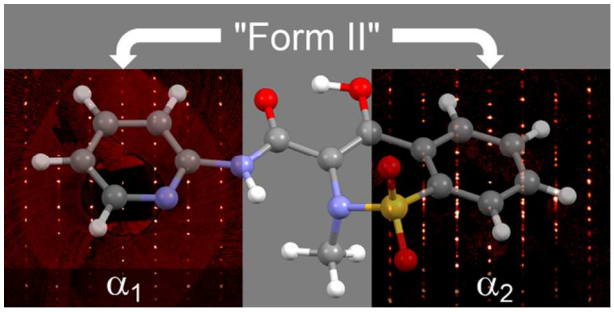

The polytypic α_1 and α_2 polymorphs of piroxicam are described and it is shown that they can be crystallized controllably.